Salty Matters

John Warren - Tuesday December 31, 2019

Stressed and flowing salt (NaCl) stands out in the diagenetic realm

Introduction

From a long-term or geological time perspective, the combination of salt's (NaCl) physical, chemical and thermal properties make it idiosyncratic when compared to the responses of most non-evaporitic sedimentary minerals and rocks in a basin. Its distinctive features mean thick subsurface salt beds in the diagenetic realm tend to dissolve or flow while carbonates and siliciclastics do not. In fact, evaporites, especially thick pure halite units (>50-80 m thick), are the weakest rocks in most deforming geosystems. Some of halites microstructural responses to stress in the diagenetic realm are more akin to structural responses in other sediments in the metamorphic realm.

However, this axiom applies only over geologic time scales, in large dimensions, and at depth (Jackson and Hudec, 2017). Time is central to understanding salt deformation at all scales from the micro to the macro. Like an ice glacier, a salt glacier (extruding sheet or namakier) is solid enough to walk, over but flows under its own weight over geologic time scales. The slower the deformation, the weaker is rock salt compared with other sedimentary rocks.

Property	Halite	Quartz	Ice
Density	2,160 kg/m^3	2,650 kg/m^3	920 kg/m^3
Bulk modulus	22 GPa	37 GPa	9 GPa
Young's modulus	29 GPa	72 GPa	9 GPa
Rigidity (shear) modulus	11 GPa	38 GPa	4 GPa
Poisson's ratio	0.31	0.17	0.33
Compressive strength	24 MPa	1,100 MPa	4 MPa
Tensile strength	2 MPa	50 MPa	1 MPa
P-wave acoustic velocity	4,200 m/s	5,800 m/s	3,800 m/s
S-wave acoustic velocity	2,400 m/s	3,750 m/s	3,100 m/s
Thermal conductivity	6.7 W/m.K	1.4 W/m.K	2.2 W/m.K
Thermal diffusivity	3.6 x 10^{-6} m^2/s	0.9 x 10^{-6} m^2/s	1.3 x 10^{-6} m^2/s
Thermal expansivity (linear)	42 x 10^{-6}/K	0.6 x 10^{-6}/K	23 x 10^{-6}/K
Melting point	801 °C	1,670 °C	0°C
Boiling point	1,466 °C	2,230 °C	100 °C

Table 1. Physical properties of halite, quartz and ice (after Jackson and Hudec, 2017)

The sample size is also critical. A cylindrical salt core held in one's hand is stiff and rigid, like an ice cube, and is likely to remain so under ambient conditions. However, a much larger cylinder of salt will deform even on a human time scale because body forces increase with the cube of the length scale. For example, a 250-m-high tower of solid salt having an average grain size of 10 mm would sag to 10 percent shorter after about a century (Janos Urai, personal communication).

The effect of compaction of clastic sediments is the third qualifier to the relative strength of salt. Before rock salt is buried, it is already a crystalline rock having the instantaneous compressive strength of concrete (Table 1). In contrast, the surrounding siliciclastic sediments have barely started to compact near the surface and consist of loose sand and mud. However, after as little as about 200 to 300 m of burial, the confining pressure strengthens siliciclastic sediments so that they become stronger than salt. Some carbonate sediments are stronger in the eogenetic realm at even shallower depths than siliciclastics and can be pervasively cemented at or just below the seafloor.

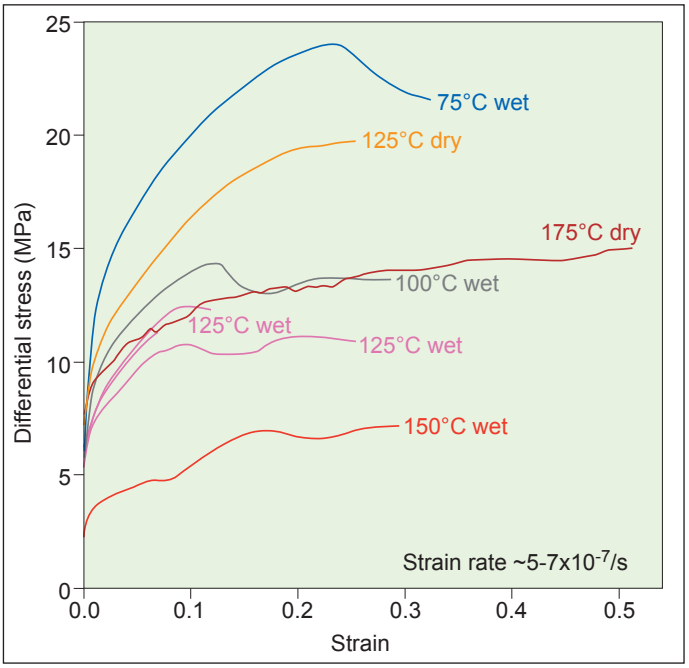

Figure 1. Rock salt weakens with increased temperature and addition of water. Stress–strain curves for wet and dry rock salt at constant strain rate of 5 × 10^{-7}/s to 7 × 10^{-7}/s and temperatures between 75 and 175 °C. After Ter Heege et al. (2005); Jackson and Hudec, 2017).

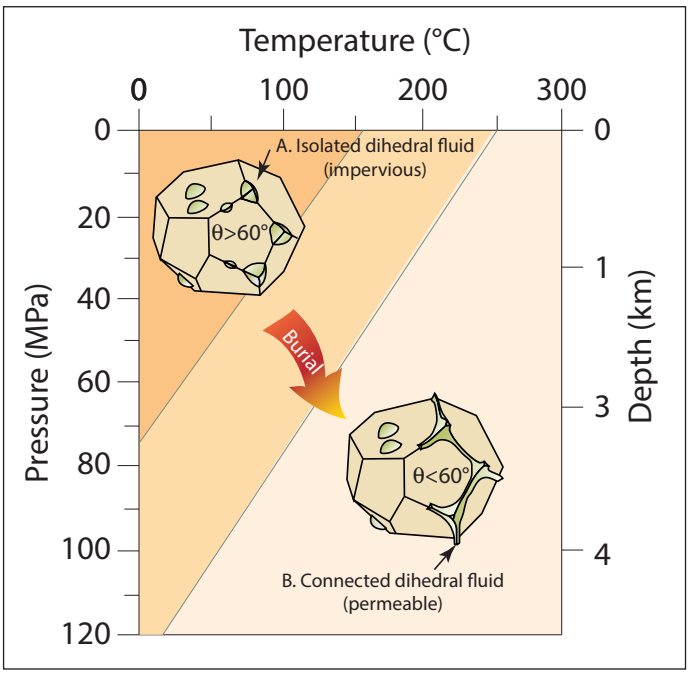

Figure 2. Effect of dihedral angle on pore connectivity in texturally equilibrated monomineralic and isotopic polycrystalline mosaic halite. Green shading shows position of dihedral fluid phase within the polyhedral intercrystalline porosity. A) Isolated porosity for dihedral angle > 60°. B) Connected polyhedral porosity for dihedral angle < 60° (after Lewis and Holness, 1996; Warren, 2016).

As siliciclastic and carbonate sediments continue to be buried, they compact, stylolitise and undergo further mesogenetic diagenesis as they lithify to sedimentary rocks, which makes them increasingly stronger than rock salt. In contrast, evaporites weaken slightly with burial as temperature rises, or as the water content of the salt increases (Figure 1). At a temperature of 125°C, dry rock has a peak flow stress of about 20 MPa, compared with about 12 MPa in damp salt of similar grain size. The presence of water films between halite grain boundaries activate solution–precipitation creep and facilitates a weakening in a deforming salt mass (see later for microstructural detail).

Later in burial, on attaining temperatures approaching metamorphic, halite undergoes another more pervasive change of intercrystalline dihedral angle converting a formerly impervious halite mass into an aquifer connected by intercrystalline polyhedral porosity (Figure 2). This thermal and pressure-induced alteration in salt texture and permeability has significant implications for the use of salt cavities in the storage of high-level nuclear waste (Warren, 2017).

Now, before we get too far into a discussion of how salt behaves unusually in the subsurface compared to non-evaporites, a little revision of Structural Geology 101 terminology is in order. Stress is a physical quantity that expresses internal forces that neighbouring particles of a continuous material exert on each other. Strain is a measure of the deformation in the material under study and is usually quantified by three axial measures defined by the strain ellipsoid – σ_1, σ_2, σ_3.

The strain ellipse is the product of a finite strain applied to a circle of unit radius. It is an ellipse whose radius is proportional to the stretch in any direction. A deformed circular object has the same shape (though not, strictly, the same size) as the strain ellipse. Mechanical strain is the mathematical expression of the shape changes resulting from mechanical stresses.

Hence the three axial strains are defined as the ratios of displacements divided by reference lengths. For the normal strain, the reference length is the initial axial length. Strain rate is the change in strain (deformation) of a material with respect to time. It comprises both the rate at which the material is expanding or shrinking (expansion rate) and also the rate at which it is being deformed by progressive shearing without changing its volume (shear rate)

In contrast, the dimension of stress is that of pressure (force/area). Therefore its magnitude is typically measured in the same units as pressure: namely, pascals (Pa) or megapascals (MPa). In the subsurface geological realm, a pascal can be considered a minimal unit and is defined as a pressure of 1 Newton exerted over a square metre. A film of water 1mm thick exerts some 10 Pa of pressure on the surface below it. The gauge pressure on the bottom of a cup of coffee is 600 - 800 Pa, and it requires 100,000 Pa to make one bar. To convert;

1 pascal (Pa) = 1 newton/m^2 (N/m^2) = 10 dynes/cm^2

= 1 x 10^{-5} bars = 9.86 x 10^{-6} atm

= 1.02 x 10^{-5} kg/m^2 = 1.02 x 10^{-9} kg/cm^2

= 1.45 x 10^{-4} psi

The megapascal (MPa) is the SI metric unit in the geological realm (1 MPa = 1 million Pa), while kPa/m is standard usage when expressing subsurface pressure gradients in the oil industry.

Density, viscosity, strength & buoyancy

After it loses effective porosity, typically by 100-200m burial, halite's density of 2.2 gm/cc remains near-constant throughout the diagenetic realm, and it is near incompressible to depths of 6-8 km (Figure 3a). With entry into near greenschist depths and pressures, deeply buried halite can experience massive recrystallisation and dissolution, along with a slight decrease in density due to thermal expansion (Figures 2, 3a; Lewis and Holness, 1996).

In contrast, burial compaction in shales and most other sediments is defined by a progressive loss of porosity, with an associated increase in density and strength until it exceeds that of the salt below. This means that salt has positive buoyancy when buried beneath non-evaporite overburden to depths in excess of a kilometre. With a muddy overburden, the depth of density crossover, sometimes called the level of neutral buoyancy, is typically shallower than 1300 to 1500 metres. It can be much shallower beneath reefs and other cemented carbonates, which can have densities equal to, or greater than, salt almost from the time of deposition. This can lead to rapid foundering and brecciation of reef materials, especially in areas of overburden extension and allochthon spreading.

Few other rocks are as thermally conductive or as close to genuinely viscous (Newtonian) as natural rock salt (Figure 3b, c). Viscosity is a measure of a fluid's resistance to flow or its internal friction and is measured by the ratio of shear stress to the rate of shear strain. Laboratory measurements show wet carnallite can have a [1]viscosity as low as 10^8 Pa.s, while dry halite has a viscosity around 10^{18} Pa.s (for comparison, honey at 14°C has a viscosity ≈ 60 Pa.s; window putty ≈ 10^5 Pa.s; and road tar ≈10^7 Pa.s. The viscosity of salt in the Gulf of Mexico is 10^{13} to 10^{17} Pa.s, depending on moisture content, crystal size and temperature. An adjacent overburden of clay or sands is less viscous by four to five orders of magnitude. Davison et al. (1996a) estimate the ratio, sedimentary rock: evaporite rock viscosity, ranges from 50 to 10^4. As different parts of a diapir deform at different rates and by different mechanisms, the effective subsurface viscosity values for diapiric salt vary with position in the diapir, the water content of the salt and time. Due to its much higher moisture content (from meteoric water infiltration), diapiric salt is much less viscous when it reaches the surface as a tongue of extruded salt than at depth.

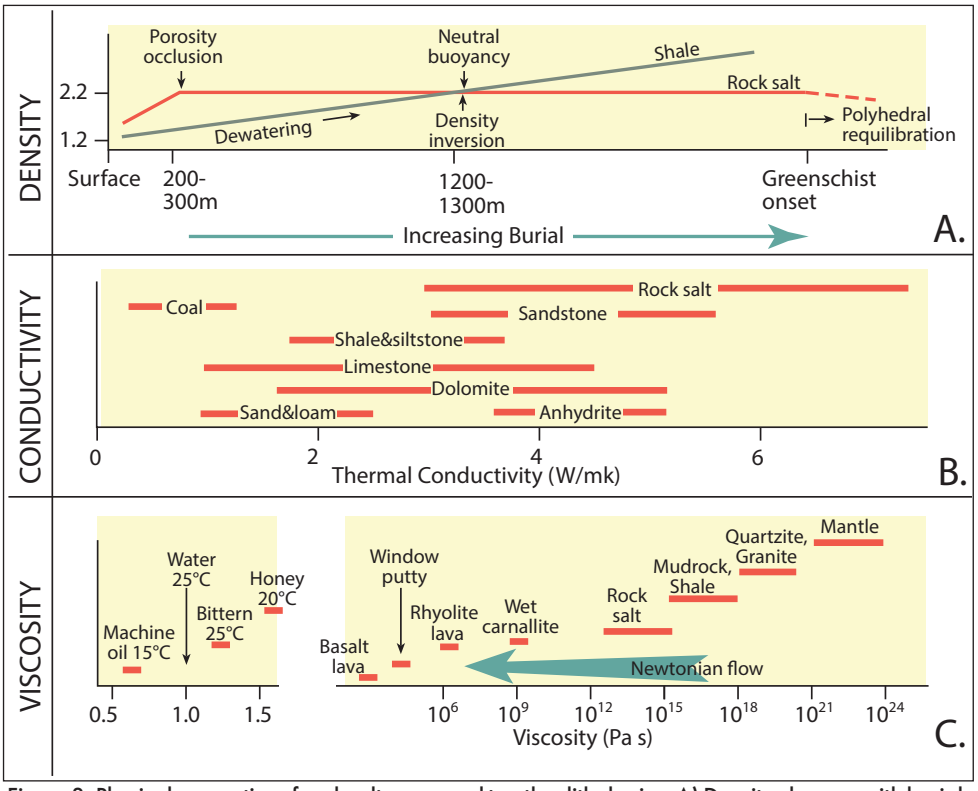

Figure 3. Physical properties of rock salt compared to other lithologies. A) Density changes with burial. B) Thermal conductivity. C) Viscosity.

Across geological time frames, finer-grained wet salt approaches [2]Newtonian viscous behaviour, unless it is atypically coarse-grained. And, like any fluid, it cannot support shear stress at geological time scales, so a mound of wet salt emplaced on the earth's surface will spread under its own weight (gravity spreading).

Using a viscous fluid model, salt diapirism and its relationship to its overburden can be likened to Rayleigh-Taylor instability with a viscous substratum (salt) and an overlying denser viscous fluid (overburden; e.g. discussions in Koyi, 1991; Talbot, 1992a,b). Under such a fluid-fluid model, diapirism is spontaneously initiated by small irregularities in the fluid-fluid interface that then amplify with time and buoyancy contrast. Diapirs rise continuously and inevitably until the less dense salt overlies its overburden. The only requirement for Rayleigh-Taylor instability in a fluid-fluid system is density inversion; diapirism modelled in such a way does not require any external trigger such as regional extension or differential loading.

Under this fluid-fluid scenario, any regional extension thins the fluid overburden and the source layer, so reducing the overall thickness. The resulting diapirs are smaller, more closely spaced, and more slowly rising than those in unthinned counterparts (Koyi, 1991). This viscosity-contrast modelling of salt flow was the dominant approach in experimental modelling in the 1980s.

Today, the "brittle school" of salt modelling dominates our thinking and experimental modelling. It considers salt as a pressurized pseudo-fluid at subsurface flow rates (i.e., Newtonian response at geological time scales). In contrast, adjacent non-evaporite sediment tends to show brittle responses to stress. In most subsurface situations this means that relative density as a trigger and a subsequent control to halokinesis, is today considered less important than relative strength of the salt unit and its overburden.

Brittle modelling of salt tectonics is better supported by geological observations that; 1) diapirs rise episodically rather than continuously, 2) that salt flows when loaded (much like toothpaste is squeezed out of its tube) and 3) that faulting, rather than folding, characterises much of the early deformation in the salt overburden. In reality, the strength response of a buried salt bed and its overburden is time dependent; its response depends on strain rate and rate of deformation in the overburden. Salt can fracture and fault at high strain rates and lower water contents (i.e., show a brittle response over short time frames). However, the required strain rate for a brittle response in salt is much higher than experienced in typical subsurface situations (Jackson and Talbot, 1994; Davison, 2009).

Subsurface non-evaporitic sediments, including indurated thick shales, show time-independent, pressure-dependent brittle behaviour under stress, and deform most readily by frictional slip

1 The SI unit of dynamic viscosity is the pascal-second (Pa·s), or equivalently kilogram per meter per second ($kg \cdot m^{-1} \cdot s^{-1}$). The CGS unit ($g \cdot cm^{-1} \cdot s^{-1} = 0.1$ Pa·s) is called the poise (P), named after Jean Léonard Marie Poiseuille.

Type of flow	Strain rate (s^{-1})	Speed (mm a^{-1})	Speed
Lava flow (faster when hotter)	10^{-5} to 10^{-4}	$5x10^{11}$ to $3x10^{13}$	1 to 60 km hr^{-1}
Ice glacier (surges with increased temperature)	10^{-10} to $5x10^{-8}$	$3x10^{5}$ to $2x10^{7}$	1 to 60 m day^{-1}
Salt glacier (surges when wet, after a rainstorm)	10^{-11} to $2x10^{-9}$	$2x10^{3}$ to $2x10^{6}$	10 to 100 km Ma^{-1}
Mantle currents (temperature and pressure controlled)	10^{-15} to 10^{-14}	10 to 10^{3}	2 m a^{-1} to 5 m day^{-1}
Spreading salt tongue (<30km wide extrusion)	$8x10^{-15}$ to 10^{-11}	2 to 20	2 to 20 km Ma^{-1}
Spreading salt tongue (>30km wide extrusion)	$3x10^{-16}$ to 10^{-15}	0.5 to 3	0.5 to 3 km Ma^{-1}
Rising diapir in stem (increases with water content)	$2x10^{-16}$ to $8x10^{-11}$	$1x10^{-2}$ to 2	10 m to 2 km Ma^{-1}

Table 2. Representative strain and flow rates (after Jackson and Vendeville, 1994).

along faults. In contrast, bedded salt under stress typically flows and deforms via folding and recrystallisation rather than fracturing. Most adherents of the brittle school contend that varying combinations of regional extension, differential loading and gravity sliding, will localise, initiate and promote diapirism of salt and shale. Conclusions of the "brittle" school are supported by studies showing virtually all sediments at shallow crustal depths (<8-10 km) deform as faulted brittle masses, rather than by the internal creep and folding that typifies deforming evaporite masses. An 8-10 km depth range encompasses much of the realm of salt tectonics in sedimentary basins.

Flow mechanisms in the diagenetic realm

Evaporite salts are unique among sediments in their tendency to flow (creep) in the diagenetic realm. Representative strain rates and speeds of salt deformation are listed in Table 2. A strain value of 10^{-15} s^{-1} indicates that a rock stretches at a rate of 10^{-15} of its length per second and is representative of the slow strain rates a value encountered in rock deformation rates in active orogenic belts. A value of 10^{-9} is 1 million times faster and represents strain rates in active (wet) salt glaciers in Iran (1.6×10^{-13} to 1.8×10^{-8} per second; Wenkert, 1979), which equates to an annual rate of rise of ≈ 2 m/year in the salt stem. But the rate of salt supply and surface flow is not constant. Salt glaciers (namakiers) in Iran always flow faster after a rain; the Dashti glacier at Kuh-e-Namak (28.26°N, 51.71°E) flows at up to 0.5 m/day during the few weeks of the annual wet season, but flows little if any during the dry season when the glacier expands and contracts diurnally in response to changes in surface temperature. The Kuh-e-Jahani salt glacier in Iran (28.60°N, 52.46°E) rises out of its orifice at 2–3 m/year, (Talbot et al. 2000), which is equivalent to a vertical strain rate of 1×10^{-11} s^{-1}. According to Davison (2009), this is close to the critical strain rate required for salt to fault.

Under enough differential stress, rocks change in shape or volume by intra-crystalline and intercrystalline processes called deformation mechanisms They include strain by diffusion of ions along grain boundaries is known as Coble creep, or stain uptake through crystals via crystal lattice dislocation and adjustment to imposed stress is known as Nabarro-Herring creep (Figure 4). Diffusion creep textures may grade into ductile grain-boundary sliding and frictional grain-boundary sliding textures. Which microstructures form at the grain scale depends greatly on the rock type: its mineralogy, impurities, intergranular fluid, grain size, fabrics, porosity, and permeability. External controls are equally important: temperature, lithostatic pressure, fluid pressure, differential stress, and externally imposed strain rate.

In all diagenetic settings, wet salt has little or no strength and so deforms by [3]diffusion creep in a fluid-like fashion. In contrast, [4]cataclastic or brittle responses to deformation, involving microfracturing and sliding of grains and grain fragments (grain crushing), are important deformation mechanisms in adjacent non-evaporite indurated sediments at low temperatures

3 Diffusion creep changes the shape and size of crystals through the movement of vacancies and atoms within crystals and along grain boundaries. Indicative textures can include equant grain shapes, indented grains, overgrowths and a lack of crystallographic preferred orientation (although preferred crystallographic orientations can also form during diffusion creep)

4 Brittle response encapsulate microfracturing, cataclasis, and frictional sliding involve the formation, lengthening, and interconnecting of microcracks; frictional sliding along microcracks and grain boundaries; and the formation and flow of pervasively fractured, brecciated, and pulverized rock and crystal fragments (micropemeability).

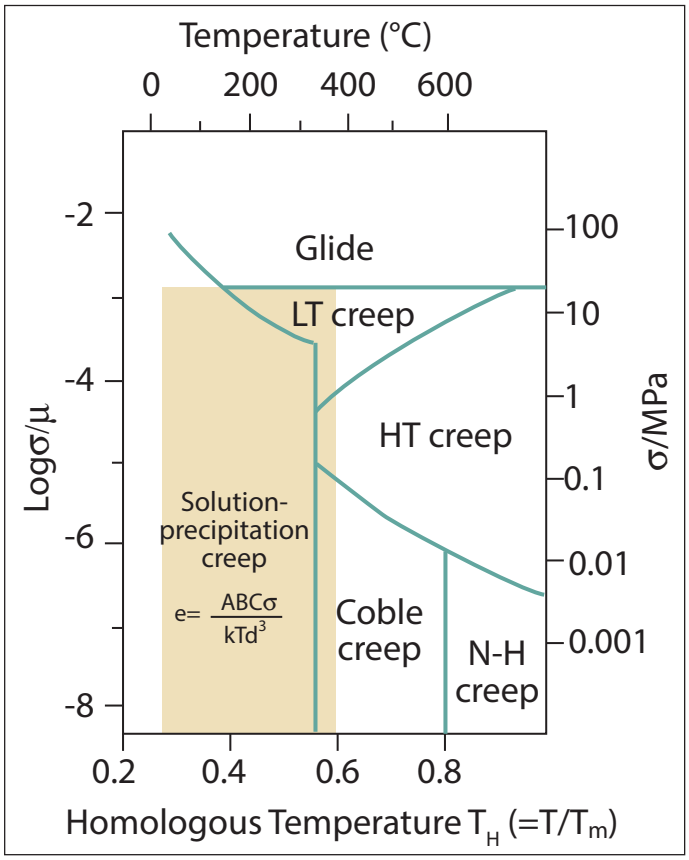

Figure 4. Diffusion mechanism map for damp rock salt showing dominant deformation mechanisms for different homologous temperatures and stresses. Shaded area shows the dominant field for most natural salt flow, which lies mainly in the solution-transfer field (solutant diffusivity terms; C = grain boundary structure parameter; k = Boltzmann constant; d = grain size. T_m = melting point of halite; LT and HT is low and high temperature; N-H is Nabarro Herring (after Urai et al., 1986).

and [5]confining pressures (Talbot and Jackson, 1987a,b; Kukla et al., 2011a, b).

For most geologic conditions in the sedimentary realm, the three main microstructural deformation processes occurring in rock salt are; A) Microcracking and cataclastic flow, B) Dislocation creep, and C) Solution–precipitation creep (Figure 5; Jackson and Hudec, 2017).

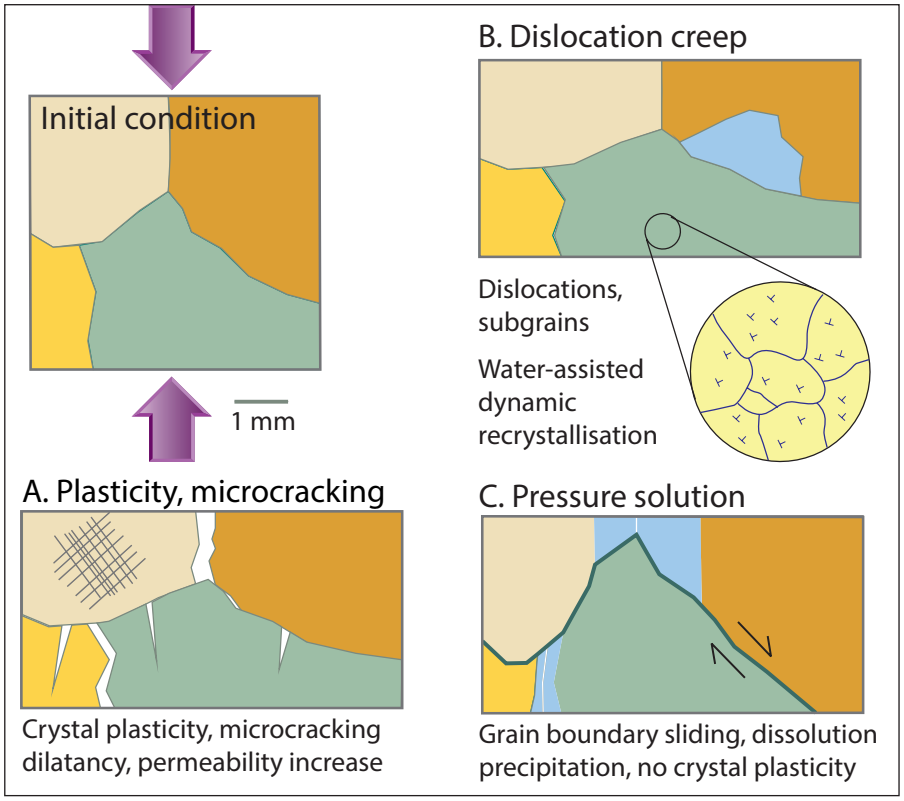

Figure 5. Crystal-scale salt deformation. A) Schematic showing the microstructural processes that can operated during the deformation of rock salt at temperatures in the range 20-200 °C. Different shades represent crystals with different orientation, blue indicates new crystals. The circular expanded inset illustrates subgrain textures (with same orientation).

Microcracking and cataclasis

Microcracking granulates rocks under low confining pressure, high strain rates, and low to moderate [6]homologous temperatures. Cataclastic flow is a brittle process in which fragments in an aggregate fracture, slide, and rotate to produce gouge, cataclasite, breccia, and voids filled by veins (Figure 4a). Cataclasis tends to increase rock volume as fractures dilate. Cataclasis dominates in halite at low temperatures, low effective confining pressures, and high differential stress. Microfractures form within grains and cut across several grains. The grains and their fragments rotate and slide past each other, dilating the rock salt and increasing its permeability. As confining pressure rises during burial, greater deviatoric stress is needed to break the rock; microcracking and dilation are suppressed, and crystal plasticity comes to dominate.

Dislocation creep

Dislocation creep is a form of crystal plasticity combining dislocation glide and dislocation recovery (Figures 4b, 5). During dislocation glide, a crystal distorts by slip along one or more weak crystallographic directions, or slip planes, where the lattice is weakly bonded. The relative positions of atoms or molecules change as slip exploits lattice defects. Eventually, dislocations can slip entirely through a crystal, which adapts its shape without distorting its lattice. As the crystal deforms, the dislocation density increases, and the moving dislocations pile up and tangle. This process increases the strain energy and causes strain hardening. To continue strain at the same differential stress, crystals must recover from their defects. Recovery is enhanced at homologous temperatures above 0.45 (Figure 4).

Kinking of crystal lattices by various combinations of slip, glide or dislocations of grains in the halite lattice itself is known collectively as dislocation creep. Based on naturally and artificially deformed salt samples, Carter and Hansen (1983) concluded dislocation creep occurs at temperatures and pressures relevant to subsurface salt deformation. They found that short-term, high-stress flow properties of dry salt can be reasonably encapsulated in an empirical power-law equation (Figure 7). This power law explains the rates of creep and [7]differential stress fields interpreted in diapiric salt. It does not explain the much higher strain rates of 10^{-8} to 10^{-11} measured in salt allochthons and salt glaciers (extruded wet salt) at stress differentials estimated to be around 0.5 MPa and at ambient surface temperatures (Talbot and Jackson, 1987a). Nor do their stress/strain triaxial experiments duplicate the elongate recrystallised textures of naturally deformed salt; such textures imply diffusional flow mechanisms (Urai et al., 1986).

Dynamic recrystallisation is syntectonic and causes dislocation sub-structured grains to rotate and boundaries to migrate (Figure 5). In subgrain rotation, which is typical of lower temperatures and stresses, dislocations are added to subgrain boundar-

5 Confining pressure describes an equal, all-sided pressure, such as lithostatic pressure produced by the weight of overlying rocks in the crust of the earth. It is considered equivalent to overburden pressure or geostatic pressure and is sometimes called vertical stress. It contrasts with the term formation pressure, which includes a pore pressure component.

6 The homologous temperature (T_H) of a crystalline material is defined as the ratio between temperature of a material (T) and the melting (solidus) temperature (T_m) in Kelvin. Because T_m of a crystalline material is controlled by the bonding force between atoms, T/T_m has been widely used to compare the creep strength of crystalline materials with different melting points. For water, with a T_m of 273 K, the homologous temperature at 0 K is 0/273 = 0, while at 0°C the T_H = 1 (273/273), and 0.5 at -100°C (137/273).
Homologous temperatures involved in creep processes are typically greater than 0.5, with creep processes becoming more active as T_H approaches 1. This is why ice glaciers can flow like salt glaciers: that is, ice deforms by creep at the high homologous temperatures of natural glaciers, as does salt.

7 Differential stress (sometimes called deviatoric stress) is any stress system where the forces acting on a unit cube are not the same in all directions, it is typically measured as $\sigma_1 - \sigma_3$..

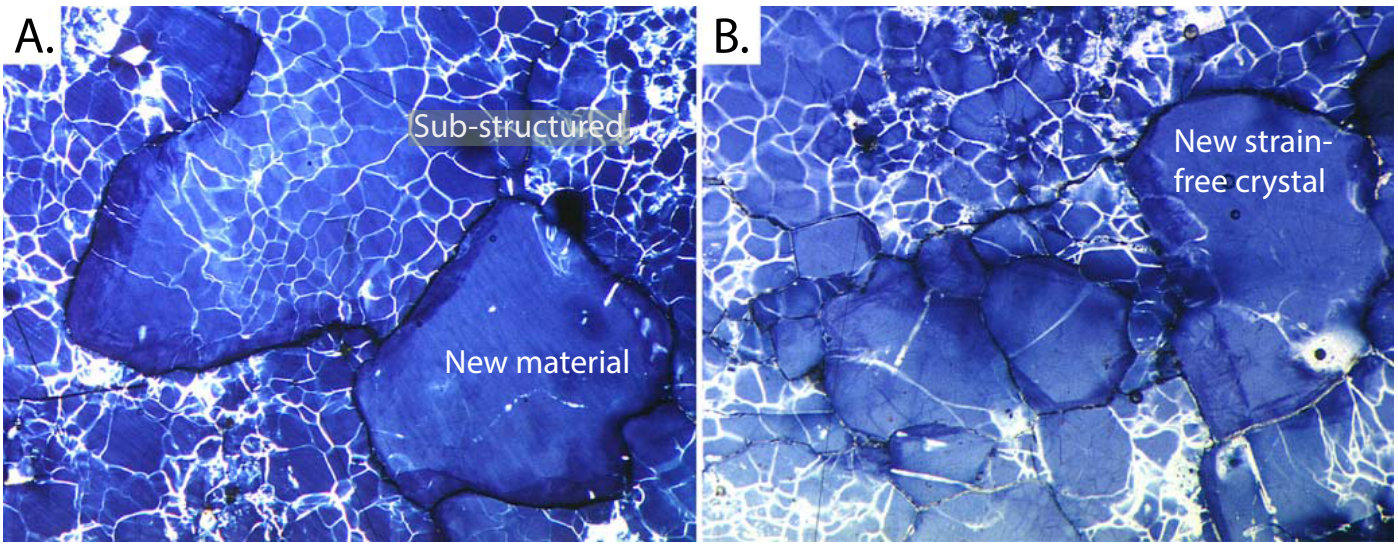

Figure 6. Deformed and irradiated Hengelo rocksalt, Germany showing the reation of subgrain microstructures and new halite crystals A) Microstructure shows subgrains (white lines), grain boundaries (dark bands), also shows clear evidence for "overgrowth" due to solution-precipitation processes such as pressure solution and and grain boundary migration. Mean grainsize in Hengelo samples is between 5 and 25 mm. Width of image is 7 mm. B) Strain-free grains that grew at the expense of deformed ones. The size of some of the new grains is comparable to that of subgrains. (Images courtesy of Janos Urai see Schléder and Urai, 2005 for details)

ies until the dislocations consolidate as a new subgrain at least 15 degrees rotated from the adjacent grain (Schléder and Urai, 2005). During grain-boundary migration, which is typical of higher temperatures and stresses, less deformed crystals grow at the expense of more deformed neighbours. Atoms of the more deformed crystal are slightly displaced to fit the less deformed lattice. Grain-boundary migration involves no strain itself, but it can allow dislocation processes to reach large strains.

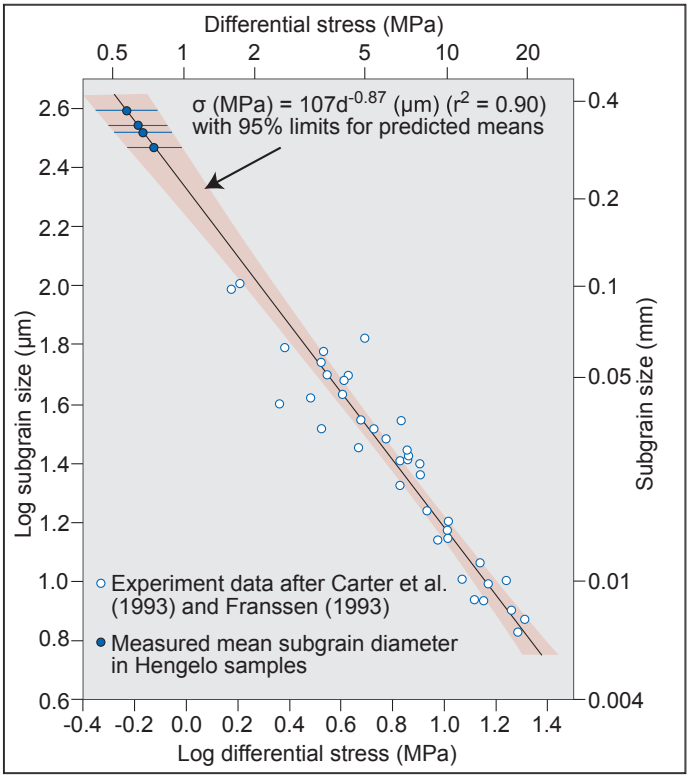

Figure 7. Differential stress is linearly proportional to subgrain size on a logarithmic plot, therefore a best-fit line of experimental data can be used to estimate paleostresses in naturally deformed rock salt (after Schléder and Urai, 2005).

Dislocation creep dominates above 100 °C at the high strain rates and differential stresses imposed in the laboratory. This crystal-plastic process allows crystals to change shape and achieve large ductile strains even at confining pressures as low as 10 MPa. As temperature and pressures rise, crystals distort further as dislocations are stacked into arrays of polygonal subgrains within larger grain (Figure 5).

As in other crystalline rocks, polygonal subgrains record the paleostress during steady-state creep because subgrain size is inversely proportional to the peak differential stress. Even for a hundred-fold range of subgrain sizes from different natural rock salts, the relationship is robust, which is the basis for estimating paleostresses in rock salt that has been naturally deformed (Figure 6). However, the effects of other variables, such as strain rate and temperature, on subgrain sizes are uncertain. Subgrain sizes in naturally deformed halite, calibrated to differential stress in the laboratory (Figure 6), indicate typical differential stress inside diapirs of less than 2 MPa and rarely as much as 5 MPa (Schléder and Urai 2005, 2007; Schléder et al. 2007). Differential stresses calculated from subgrains are about twice as high in the crests of emergent diapirs of Ara salt (Oman) as in the source layer of the same rock salt (Schoenherr et al. 2009).

When differential stress declines, if the rock is still hot, static recrystallization anneals subgrains, heals dislocations, and removes dislocation tangles and other defects. Grain boundaries straighten to form polygonal grains that enlarge.

Pressure solution

During pressure solution, halite grain boundaries dissolve where they impinge at points of high normal stress, which increases solubility (Figure 4c). Dissolved ions diffuse by solution transfer through a fluid film on the grain boundary and precipitate where differential stress is lower. By this combination of water-assisted processes, known as solution–precipitation creep, grains change

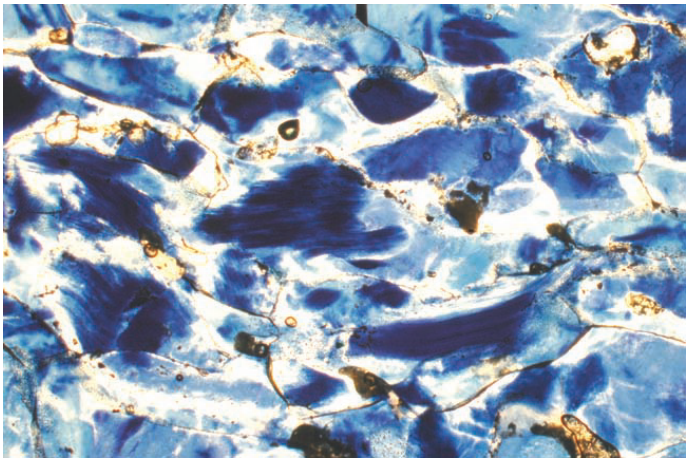

Figure 8. Typical microstructure of solu-tion-precipitation deformation in glacier salt from Iran, as observed in gamma-irradiated sections (after Schléder and Urai 2007). Micro-structures such as oriented fibrous overgrowths on both sides of a grain boundary, growth banding and the absence of slip lines or subgrains suggest that the principal deformation mechanism was solu-tion-precipitation creep accompanied by grain boundary migration and grain boundary sliding. Crystal fabrics measured by EBSD in these samples show only a weak crystallographic preferred orientation consistent with solution-precipitation accommodated grain boundary sliding. Image width is 4 mm.

shape without internal strain (Figure 8). This creep operates at moderate homologous temperatures and relatively low strain rates; a pore fluid must be present.

Most natural salt samples contain minute traces (>10–20 ppm) of saturated brine as intracrystalline inclusions or grain-boundary films (Roedder, 1984). The fluid was trapped during deposition or diagenesis of the salt beds or percolated in as meteoric water into extrusive salt. During geologic deformation (where strain rates and differential stresses are low), microstructural processes at grain boundaries are significant in deforming damp rock salt (Urai et al. 2008).

Solution–precipitation creep is driven by differences in chemical potential across grain boundaries resulting from differences in dislocation density (Jackson and Hudec, 2017, and references therein). Ions dissolve from a highly strained grain and diffuse through the fluid film, driven by loss of chemical potential. Eventually, the ions precipitate against a less strained grain under lower differential stress, allowing the grain to enlarge. Ions migrate at rates of as much as 10 nm/s at room temperature. Precipitation in low-stress zones can compact porous rock salt and fill gaps that would otherwise form during grain-boundary sliding.

During grain-boundary sliding, grains slide past each other without creating significant voids because diffusion (through crystal lattices or along their boundaries, or through a pore fluid) continually adjusts the shapes of grains to fit the changing neighbours. The microstructure changes little despite large ductile strains in the rock as a whole. Grain-boundary sliding acts during rapid strain rates at low differential stress in fine-grained rocks. Such conditions dominate the extrusion of salt sheets, so the mechanism is important in this context (Figure 8).

The process of solution transfer creep in deforming salt produces new gneiss-like crystal textures made up of amoeboid-like strain-free flattened salt grains, showing flow-parallel fabrics. Solution-transfer creep or pressure solution creep occurs in regimes of differential stress where halite grains dissolve in regions of high stress and reprecipitate in regions of low stress (aka strain shadows). The basic processes involved are the migration of existing grain boundaries and the formation of new high angle grain boundaries (Drury and Urai, 1990). New crystals are less sub-structured and replace older more substructured grains as migrating crystal grain boundaries consume and sweep through the older milky inclusion-rich portions of the salt (Schenk and Urai, 2004). Much of this new salt is clear and sparry, rather than milky from intracrystalline inclusions.

The high solubility of chloride salts means pressure solution creep (aka solution precipitation creep, solution transfer creep, or stress-induced solution transfer) is the prevalent deformation mechanism in wet salt flowing in the shallow diagenetic temperature realm (Figures 4c, 8; Urai et al., 1986, 2008). That is, diffusion mechanisms can operate at much lower temperatures and differential stresses in wet salt than in non-salt rock types, where temperatures measured in hundreds of degrees are more typical of diffusion.

Flow Laws

Figure 9 compares the strain rates of solution–precipitation creep and dislocation creep in damp halite at a temperature of 50 °C. According to Jackson and Hudec (2017), this graphs almost all that a nonspecialist needs to know about the variable rheology and deformation mechanisms of pure rock salt. The blue line for dislocation creep is based on experimental data between strain rates of about 1^{-10}/s and 10^{-7}/s (Schléder and Urai 2005; Urai et al. 2008). The line is extrapolated to a low geologic strain rate of 10^{-15}/s. Dislocation creep is insensitive to grain size, whereas solution–precipitation creep, shown by the purple lines, is highly sensitive to grain size. Fine-grained halite deforms several orders of magnitude faster by solution-precipitation creep than does coarse-grained halite at the same differential stress. For example, at a differential stress of 1 MPa, fine-grained (0.1-mm) halite takes 23 days to reach 10 percent strain, whereas coarse-grained (10-mm) halite takes 160,000 years. The line for dislocation creep obliquely crosses the lines for solution–precipitation creep. At each crossing point, the two types of creep are equally effective. For example, for a 10-mm grain size, the two mechanisms are equal at a strain rate of about 3×10^{-13}/s and differential stress of about 3 MPa.

Figure 9 shows that salt deforms by both solution-precipitation creep and climb-controlled dislocation creep during diapirism (aided by water-assisted dynamic recrystallization). Solution–precipitation creep dominates in extrusive salt sheets because the salt is typically damp and fine grained, and because deformation in salt sheets is driven by low differential stress (Jackson and Hudec, 2017). Conversely, dislocation creep and solution–precipitation creep contribute roughly equally to the strain rate in salt stocks.

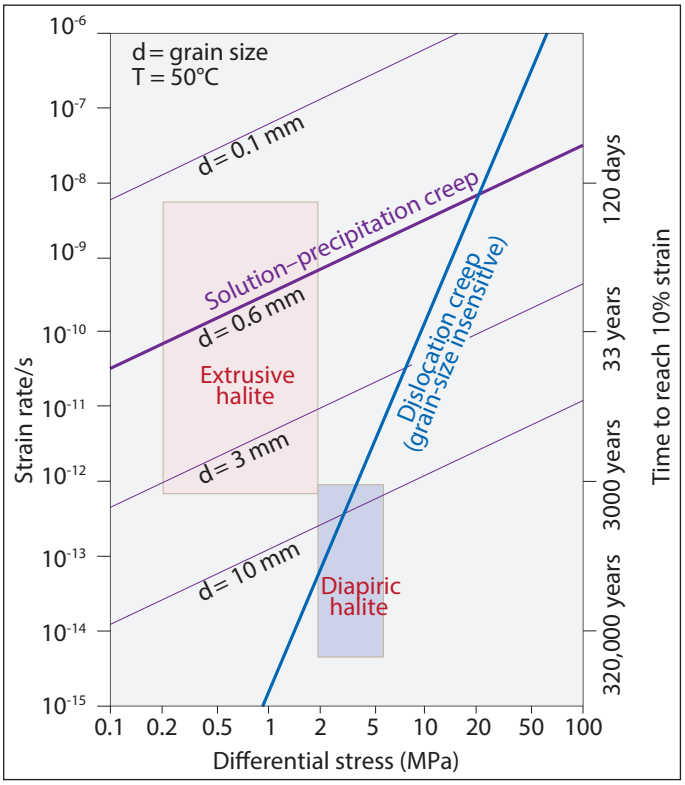

Figure 9. The stress–strain-rate fields for salt diapirism and salt extrusion are compared with the two main flow laws for damp, pure halite, based on experiments. Solution–precipitation creep dominates in extrusive salt glaciers, although the time taken to reach 10 percent strain ranges from a few weeks (in fine-grained salt) to more than 300,000 years (in coarse-grained salt). In contrast, dislocation creep is insensitive to grain size. The line for dislocation creep obliquely crosses lines for solution–precipitation creep, at which points the two types of creep are equally effective under a wide range of grain sizes, differential stresses, and strain rates. The most significant crossing point, however, is in the field for diapirism (pink), where stress is about 3 MPa, strain rate is about 10^{-13}/s, and grain size is 10 mm. After Urai et al. (2008).

Microstructural evolution

A sequence of deformation mechanisms controls the micro-structures in different parts of a salt structure (Figure 10; Jackson and Hudec, 2017). During rise inside a salt stock, the increasing differential stress forms subgrains by dislocation within the porphyroclasts, although they appear clear to the naked eye (Figure 10a; Urai and Spiers 2007; Desbois et al. 2010). At this stage, the proportion of subgrains is small enough for one to call the rock salt protomylonite. As diapiric salt rises to the summit, it diverges and differential stress declines. As meteoric water seeps in, the exposed salt begins to recover and dynamically recrystallise as grain boundaries migrate and create abundant growth bands in the growing grains (Figure 10b; Desbois et al. 2010). Dominant dislocation creep in the upstream and middle parts of a salt glacier transitions to dominant water-assisted grain-boundary sliding in the downstream region. Remnants of porphyroclasts contain subgrains, fluid-inclusion bands, and perpendicular sets of dark bands, which survive from where they formed in the diapir under high stresses (Figure 10c). The porphyroclasts become smaller and fewer downslope as they disperse within increasing volumes of fine-grained daughter grains in the groundmass (Figure 10d; Talbot 1981). The small daughter grains lack subgrains and form by solution–precipitation creep at differential stresses of only 0.2 to 1.0 MPa and temperatures of 20 to 40 °C.

Because of the variable grain size, strain rates in salt glaciers are likely to vary greatly within deforming salt masses as strain concentrates in fine-grained mylonites. Using a metaphor of melting ice cream, Jackson and Hudec (2017) describe this situation as if melting occurs in thin layers. These thin melting layers of ice cream allow much faster flow than is possible in the stronger interlayers. Reduction of grain size allows the salt glacier to advance rapidly by deformation of its weakest layers – the mylonites – while the interbedded protomylonites deform more slowly but are carried along in the downslope flow.

Permeability changes in rock salt in the diagenetic realm

The association of evolving textures illustrated in figure 10shows a commonality of low permeability in almost all stages of diagenetic alteration from the time of shallow burial of the salt bed, throughout its subsurface evolution, flow and décollement and into the time of its return to the surface as diapirs, allochthon sheets and namakiers (Warren 2016, Chapter 10). Evaporites are thought to form a perfect seal for hydrocarbons for three reasons (Schoenherr et al. 2007a, b). First, there is an ongoing near-isotropic stress state in salt (equivalent to a highly viscous fluid) that generally resists hydrofracturing because differential stress is relatively low (Hildenbrand and Urai 2003). Second, permeability and porosity of crystalline rock salt typically are very low in the diagenetic realm, even after only 70 m of burial (Casas and Lowenstein 1989). Third, permanent deformation of rock salt in nature is generally ductile and nondilatant (Jackson and Hudec, 2017). For these reasons, intact rock salt has an extremely low permeability ($<10^{-9}$ md) unless impurity zones, such as shale or carbonate stringers, facilitate fluid entry (Warren 2017; Figure 11).

For fluid pressure to have an effect on rocksalt permeability, the fluid must first penetrate, which is difficult where rock salt is tight and crystalline. However, two processes can increase rock salt permeability in the diagenetic realm (Schoenherr et al. 2007a, b): (1) microcracking and associated dilation and, 2) a network of brine-filled pores and triple-junction tubes between halite grains in deeply buried rock salt.

During dilatant microcracking of rock salt, its permeability increases by as much as six orders of magnitude. Rock salt can dilate in the walls of salt caverns in a damage zone that can penetrate as much as a few meters into the mine or cavity wall, so facilitating rock bursts (Warren, 2017). In some abandoned solution-mining caverns, fluid pressures in the cavern approach lithostatic levels after the cavern walls have converged. As a result of the high fluid pressure and low effective stress, the cavern roof dilates and leaks fluids (Fokker et al. 1995). Under triaxial deformation where fluid pressure slowly increases, rock salt becomes more permeable as grain-boundary cracks form (Lux 2005).

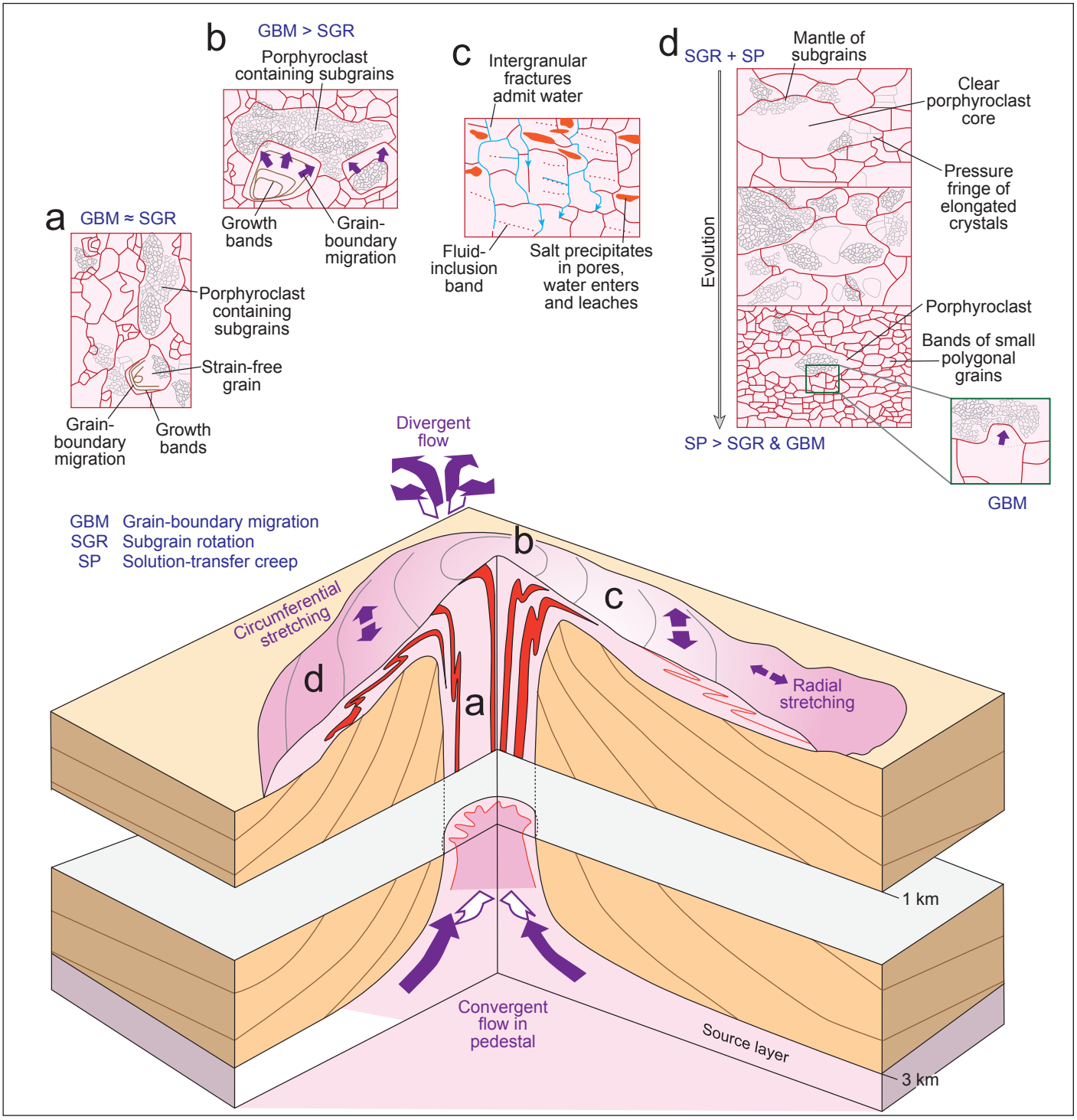

Figure 10. Deformation mechanisms and microstructures differ within a salt stock and a salt sheet. The diagram illustrates complex changes occurring as salt converges from the source layer, rises up a diapir's stem, then diverges and extrudes glacially downhill. GBM = grain-boundary migration; SGR = subgrain rotation; SP = solution-transfer creep (after Desbois et al., 2010; Jackson and Hudec, 2017).

In some situations of hydrocarbon generation in salt-encased maturing source rocks, fluid pressure can rise to where it is nearly equal to lithostatic pressure, rock salt then dilates and microfractures, creating permeability and allowing the entry of fluids (Warren, 2017). This process has formed black salt haloes around organic-rich salt encased Ara carbonate "sliver" reservoirs in the South Oman Salt Basin (Figure 12; Kukla et al. 2011a, b). These carbonate bodies are isolated in salt and frequently contain low-permeability dolomites. Such reservoirs are characterized by high initial hydrocarbon production rates due to hard [8]overpressures, followed by rapid pressure drops. But not all

8 The term hard over pressure is an often misunderstood term, dating back to Loucks, et al (1979), who recognized three pressure regimes that they defined in terms of pressure-depth gradients:
a) Normal pressure (0.465 psi/ft, 8.9 PPG equivalent mud weight, 1.07 kg/l),
b) Soft overpressure (0.465 to 0.700 psi/ft, 13.5 PPG equivalent mud weight, 1.62 kg/l), and
c) Hard overpressure (> 0.700 psi/ft, 13.5 PPG equivalent mud weight, 1.62 kg/l)
The term hard overpressure is also mis-used without reference to pressure gradient to describe narrow transition zones (as often typifies overpressure transitions in the immediate vicinity of a salt seal)

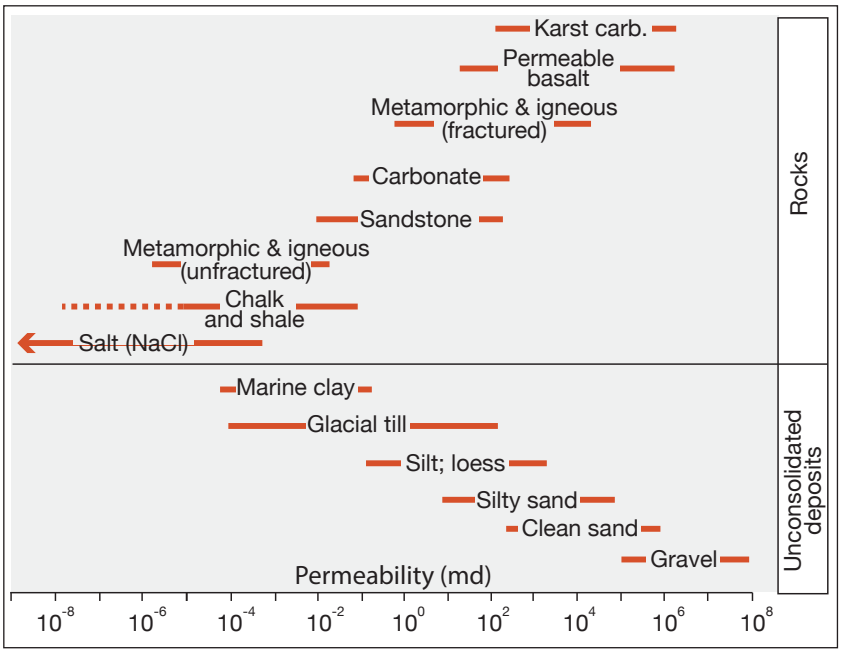

Figure 11. Permeability ranges of typical rocks and sediments, including rock salt (after Warren, 2016)

stringers are overpressured and a temporal relationship, defined by increasingly overpressured reservoirs within stratigraphically younger units, is observed. There are two distinctly independent pressure trends in the Ara stringers; one is hydrostatic to slightly-above hydrostatic, and the other is overpressured from 17 to 22 kPa.m^{-1}, almost at lithostatic pressures (Figure 13a).

The black staining of the halite is caused by intragranular microcracks and grain boundaries filled with solid bitumen formed by the alteration of oil (Figure 14a-c). The same samples show evidence for crystal plastic deformation and dynamic recrystallization. Subgrain-size piezometry indicates a maximum differential palaeostress of less than 2 MPa. Under such low shear stress, laboratory-calibrated dilatancy criteria indicate that oil can only enter the rock salt at near-zero effective stresses, where fluid pressures are very close to lithostatic.

In Schoenherr et al.'s (2007b) model, the oil pressure in the carbonate stringer reservoirs reservoir increases until it is equal to the fluid pressure in

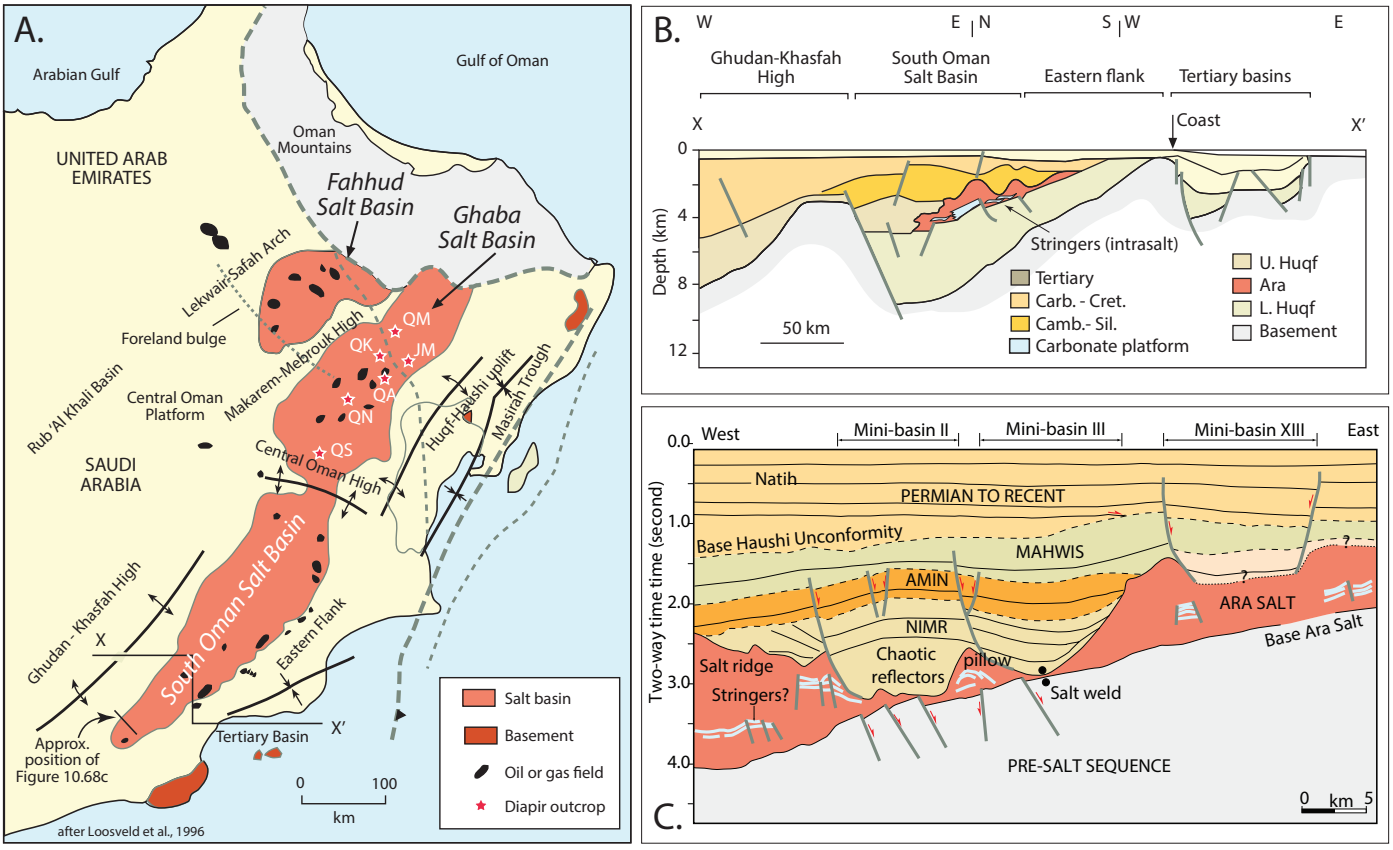

Figure 12. Salt Basins of Oman. A) Map view of three main salt basins. Palaeozoic strata capping the Ghaba Salt Basin and along the eastern flank of the South Oman Salt Basin are the main oil and gas producers, not Neoproterozoic platform carbonates or Athel Fm. silicilyte slivers, which host stringer reservoirs more toward the centre of the South Oman Salt Basin. Location of the six surface-piercing salt domes in the Ghaba Salt Basin (indicated by star) are: Qarn Sahmah (QS), Qarat Kibrit (QK), Qarat Al Milh (QM), Qarn Nihayda (QN), Qarn Alam (QA) and Jebel Majayiz (JM). B) Cross section (x-x') through the South Oman Salt Basin, schematically showing position of carbonate platform and stringers in the Ara Salt (after Loosveld et al., 1996 and Schröder et al., 2000a, b). C) Section (seismic overlay) showing interrelationship between overburden loading (minibasins II, III and XIII) and distribution of carbonate reservoir stringers within the halokinetic Ara salt (after Al-Barwani and McClay, 2008).

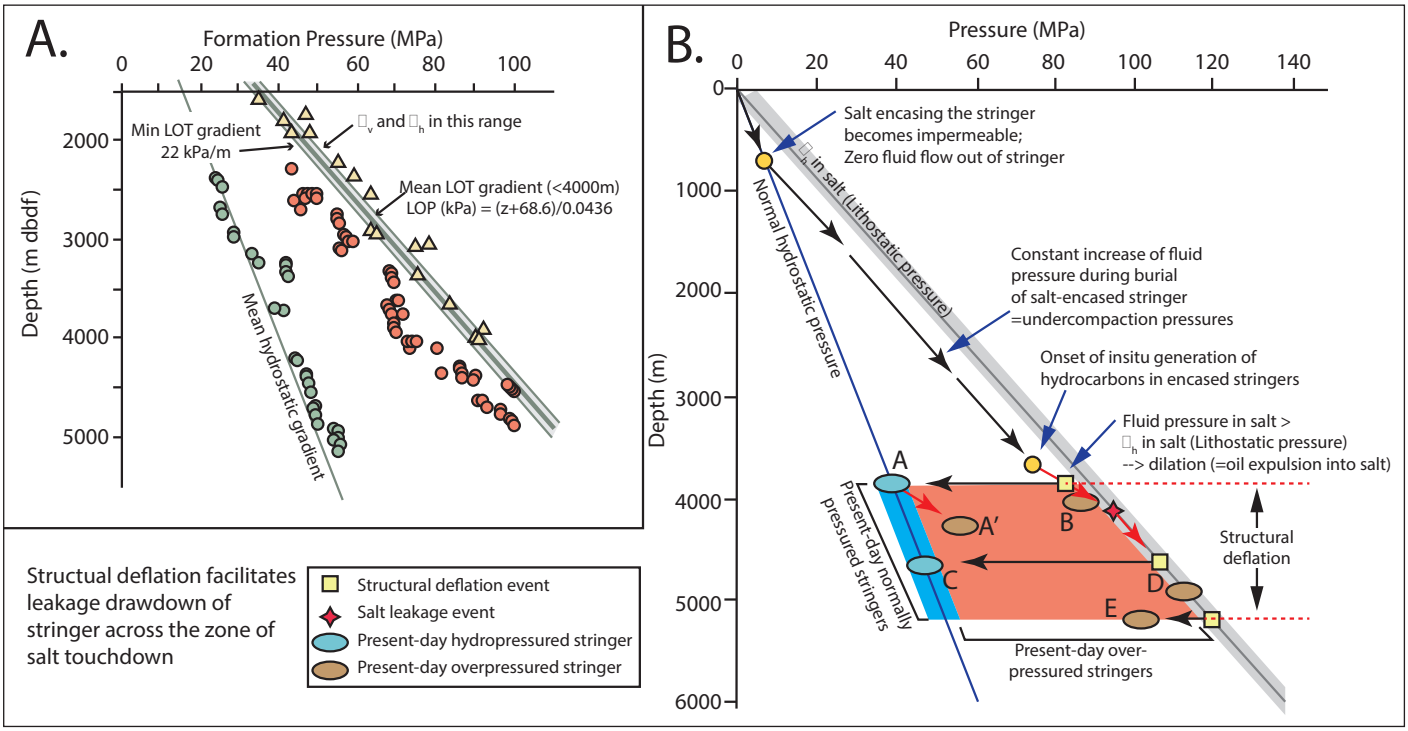

Figure 13. Overpressure in the carbonate stringers of the South Oman Salt Basin (after Kukla et al., 2011a, b). A) Measured formation pressures in the Ara carbonates (circles) versus depth. The plot shows two different pressure populations: one at near-hydrostatic pressures, with a mean pore-pressure coefficient λ= 0.49 (green circles), and one at near-lithostatic pressures, with a mean pore-pressure coefficient λ = 0.87 (grey circles). Brown triangles are leakoff test (LOT) data, and z is depth in metres. The thick black band represents the range of differential stress difference (σ_1–σ_3 [maximum principal stress - minimum principal stress]) in rock salt as derived from integrated density logs and subgrain size piezometry. tvdbdf = true vertical depth below derrick floor. B) Schematic illustrating mechanisms of overpressure generation and pressure deflation in the Ara Stringers through the burial process (see text for detail).

the low but interconnected porosity of the Ara Salt, plus the capillary entry pressure (Figures 13b, 15). When this condition is met, oil is expelled into the rock salt, which dilates and increases its permeability by many orders of magnitude. Sealing capacity is lost, and fluid flow will continue until the fluid pressure drops below the minimal principal stress, at which point rock salt will reseal to maintain the fluid pressure at lithostatic values.

Inclusion studies in the halite indicate ambient temperatures at the time of entry were in excess of 90°C, implying hydrocarbons could move into polyhedral interconnected tubes in the halite. These conduits were created in response to changes in the polyhedral angle in the halite in response to elevated temperatures (Lewis and Holness, 1995).

Hydrocarbon-stained "black salt" can extend up to 100 metres from the pressurised supplying stringer into the Ara salt (Figure 14, 15). It indicates a burial-mesogenetic pressure regime and is not the same process set as seen in the telogenetic "black salt" regions of the onshore Gulf of Mexico. The latter are created by dissolution, meteoric water entry, and clastic contamination, as in the crests of nearsurface diapirs such as Weeks Island (Warren, 2017). An Ara stringer enclosed by oil-stained salt but now below the lithostatic gradient likely indicates a later deflation event that caused either complete (C) or partial (E) loss of overpressures. Alternatively, stringers showing overpressure, but below the lithostatic gradient (E), might be explained by regional cooling or some other hitherto unexplained mechanism (Figure 13b; Kukla et al., 2011a, b).

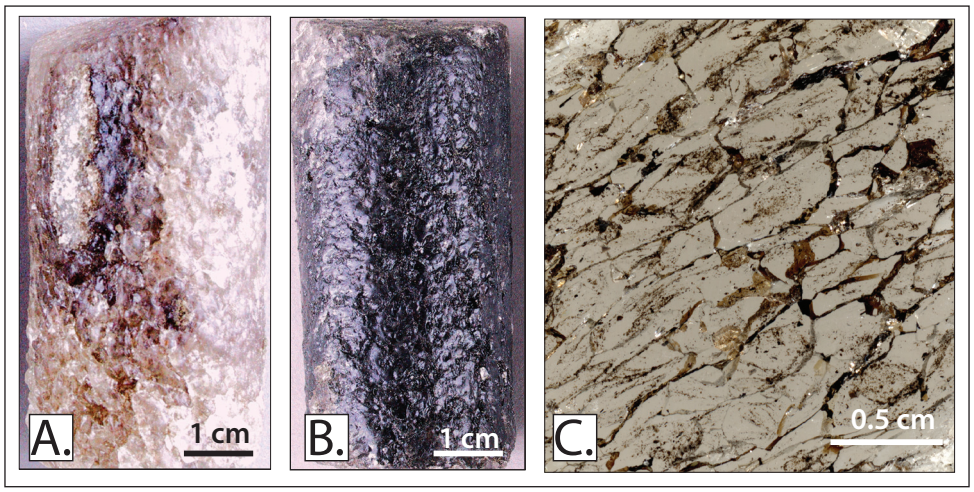

Figure 14. Hydrocarbon-impregnated halite ("black halite") from the Ara Salt, South Oman Salt basin. A) Lightly impregnated salt core, B) Heavily impregnated zone in salt core, this is classic Omani "black salt". C) Photomicrograph of naturally-impregnated salt showing interconnected polyhedral porosity outlined by the darker hydrocarbons (all images courtesy of Janos Urai; see Schoenherr et al., 2007b).

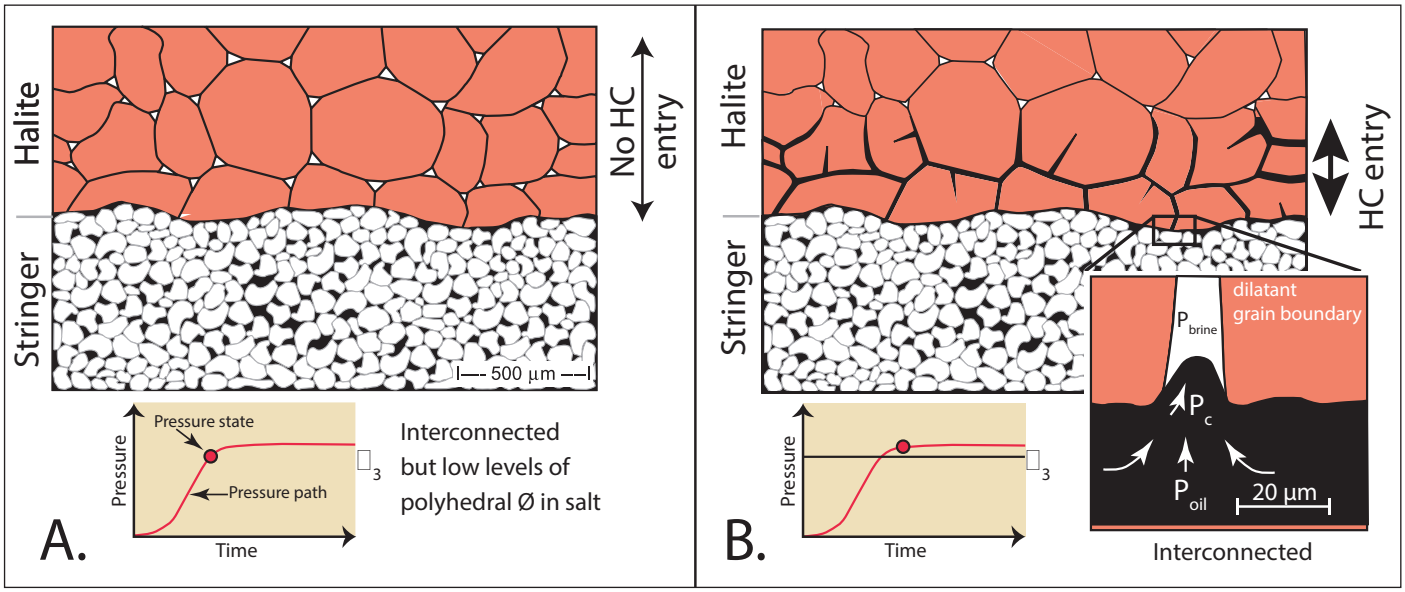

Figure 15. Entry of pressurised hydrocarbons (HC) into polyhedral salt pores. A) schematic cross section in (a) shows the interface of stringer reservoir and Ara Salt. Halite has an interconnected but low porosity represented by the triangular white spaces between the salt crystals (cut perpendicular to the triple junction tubes - thermal response in salt). The red dot in the schematic pressure-versus-time diagram indicates that the oil pressure (P_{oil}) is equal to σ_3 in the Ara Salt. B) Because of overpressure buildup, P_{oil} in the stringer exceeds the minimum principal stress (σ_3) of the salt by the capillary entry pressure (P_c), allowing the entry of oil into the triple junction tubes of the salt, leading to a diffuse dilation of the Ara Salt by grain boundary opening and intracrystalline microcracking (After Schoenherr et al., 2007b).

Structural, petrophysical and seismic data analysis suggests that overpressure generation in the Ara is driven initially by fast burial of the stringers in salt, with a subsequent significant contribution to the overpressure from thermal fluid effects and kerogen conversion of organic-rich laminites with the stringer bodies. If the overpressured stringers come in contact with a siliciclastic minibasin, they will deflate and return to hydrostatic pressures (A) in Figure 13b. When the connection between the minibasin and the stringers is lost, they can regain overpressures because of further oil generation and burial (A'). If hydrocarbon generation in undeflated stringers stops relatively early, the fluid pressures do not reach lithostatic pressures (B). If hydrocarbon generation continues, the fluid pressures exceed the lithostatic pressure (red star), leading to dilation and oil expulsion into the rock salt to what is locally known as "black salt" (D and E).

Salt's responses are unusual across the diagenetic realm

This article has focused on halite and its exceptional properties. Halite rock salt is the main constituent in halokinetic structures, which play a fundamental role in the creation of many metal and hydrocarbon traps (Warren, 2016). Much of salt's ability to trap and enrich accumulations of a variety of commodities (oil, gas, copper, lead, zinc) in the diagenetic realm is related to its extreme rheological weakness. Most other sediments tend to crack and fracture in the same stress fields where rock salt tends to flow and recrystallise into any strain shadows. This allows subsurface salt to maintain its seal capacity until it is leached by undersaturated crossflows of a variety of basinal and hydrothermal waters.

Not only is rock salt one of the weakest and most consistently impermeable sediments in the diagenetic realm, its high thermal conductivity makes halokinetic salt a driver for circum-diapir fluid convection and alteration. As well, salt stems can enhance or deplete geothermal gradients in the vicinity of salt stems and allochthon sheets (Warren 2016, Chapter 8). Throughout rock salt's time in the diagenetic realm, it not only tends to flow while maintaining seal capacity, it also tends to dissolve from its edges inward, so supplying a range of chemical modifications to the ionic proportions, densities and temperature fields in the sediments and pore waters adjacent to bedded and halokinetic structures.

References

Al-Barwani, B. and McClay, K., 2008. Salt tectonics in the Thumrait area, in the southern part of the South Oman Salt Basin: Implications for mini-basin evolution. GeoArabia, 13(4): 77-108.

Carter, N.L. and Hansen, F.D., 1983. Creep of rocksalt. Tectonophysics, 92(4): 275-333.

Casas, E. and Lowenstein, T.K., 1989. Diagenesis of saline pan halite; comparison of petrographic features of modern, Quaternary and Permian halites. Journal of Sedimentary Petrology, 59(5): 724-739.

Davison, I., 2009. Faulting and fluid flow through salt. Journal of the Geological Society, 166(2): 205-216.

Desbois, G., Zavada, P., Schléder, Z. and Urai, J.L., 2010. Deformation and recrystallization mechanisms in actively extruding salt fountain: Microstructural evidence for a switch in deformation mechanisms with increased availability of meteoric water and decreased grain size (Qum Kuh, central Iran. Journal of Structural Geology, 32: 1-15.

Drury, M.R. and Urai, J.L., 1990. Deformation-related recrystallization processes. Tectonophysics, 172: 235-253.

Fokker, P.A., Urai, J.L. and Steeneken, P.V., 1995. Production-induced convergence of solution mined caverns in magnesium salts and associated subsidence. In: F.B.J. Barends, F.J.J. Brouwer and F.H. Schröder (Editors), Land subsidence: Natural causes, measuring techniques, the Groningen gas field: Proceedings of the Fifth International Conference on Land Subsidence, Den Haag, Netherlands, pp. 281-289.

Hildenbrand, A. and Urai, J.L., 2003. Investigation of the morphology of pore space in mudstones – First results. Marine and Petroleum Geology, 20: 1185-1200.

Jackson, M.A. and Hudec, M., 2017. Salt Tectonics: Principles and Practice. Cambridge University Press, Cambridge.

Jackson, M.P.A. and Talbot, C.J., 1994. Advances in salt tectonics. In: P.L. Hancock (Editor), Continental deformation. Pergamon Press, Tarrytown, NY, pp. 159-179.

Jackson, M.P.A., Vendeville, B.C. and Shultz-Ela, D.D., 1994. Structural dynamics of salt systems. Annual Review of Earth and Planetary Sciences, 22: 93-117.

Koyi, H.A., 1991. Gravity overturns, extension, and basement fault activation. Journal of Petroleum Geology, 12: 117-242.

Kukla, P., Urai, J., Warren, J.K., Reuning, L., Becker, S., Schoenherr, J., Mohr, M., van Gent, H., Abe, S., Li, S., Desbois, Zsolt Schléder, G. and de Keijzer, M., 2011a. An Integrated, Multiscale Approach to Salt Dynamics and Internal Dynamics of Salt Structures. AAPG Search and Discovery Article #40703 (2011).

Kukla, P.A., Reuning, L., Becker, S., Urai, J.L. and Schoenherr, J., 2011b. Distribution and mechanisms of overpressure generation and deflation in the late Neoproterozoic to early Cambrian South Oman Salt Basin. Geofluids, 11(4): 349-361.

Lewis, S. and Holness, M., 1996. Equilibrium halite-H2O dihedral angles: High rock salt permeability in the shallow crust. Geology, 24(5): 431-434.

Loosveld, R.J.H., Bell, A. and Terken, J.J.M., 1996. The Tectonic Evolution of Interior Oman. GeoArabia, 1(1): 28-51.

Loucks, R.G., Richmann, D.L. and Milliken, K.L., 1979. Factors controlling porosity and permeability in geopressured Frio sandstone reservoirs, General Crude Oil-Dept. of Energy Pleasant Bayou Test Well, Brazoria County, Texas, Fourth Geopressured-Geothermal Energy Conf., Univ. of Texas, Austin.

Lux, K.-H., 2005. Long-term behaviour of sealed liquid-filled salt cavities – A new approach for physical modelling and numerical simulation – Basics from theory and lab investigations. Erdöl Erdgas Kohle, 121: 414-422.

Roedder, E., 1984. The fluids in salt. American Mineralogist, 69(5-6): 413-439.

Schenk, O. and Urai, J.L., 2004. Microstructural evolution and grain boundary structure during static recrystallization in synthetic polycrystals of sodium chloride containing saturated brine. Contributions to Mineralogy and Petrology, 146: 671-682.

Schléder, Z., Burliga, S. and Urai, J.L., 2007. Dynamic and static recrystallization-related microstructures in halite samples from the Kłodawa salt wall (central Poland) as revealed by gamma-irradiation. Neues Jahrbuch für Mineralogie - Abhandlungen: Journal of Mineralogy and Geochemistry, 184(1): 17-28.

Schleder, Z. and Urai, J.L., 2005. Microstructural evolution of deformation-modified primary halite from the Middle Triassic Rot Formation at Hengelo, The Netherlands. International Journal 0f Earth Sciences, 94(5-6): 941-955.

Schleder, Z. and Urai, J.L., 2007. Deformation and recrystallization mechanisms in mylonitic shear zones in naturally deformed extrusive Eocene-Oligocene rocksalt from Eyvanekey plateau and Garmsar hills (central Iran). Journal of Structural Geology, 29(2): 241-255.

Schoenherr, J., Littke, R., Urai, J.L., Kukla, P.A. and Rawahi, Z., 2007a. Polyphase thermal evolution in the Infra-Cambrian Ara Group (South Oman Salt Basin) as deduced by maturity of solid reservoir bitumen. Organic Geochemistry, 38(8): 1293-1318.

Schoenherr, J., Reuning, L., Kukla, P.A., Littke, R., Urai, J.L., Siemann, M.G. and Rawahi, Z., 2009. Halite cementation and carbonate diagenesis of intra-salt reservoirs from the Late Neoproterozoic to Early Cambrian Ara Group (South Oman Salt Basin). Sedimentology, 56(2): 567-589.

Schoenherr, J., Urai, J.L., Kukla, P.A., Littke, R., Schleder, Z., Larroque, J.-M., Newall, M.J., Al-Abry, N., Al-Siyabi, H.A. and Rawahi, Z., 2007b. Limits to the sealing capacity of rock salt: A case study of the infra-Cambrian Ara Salt from the South Oman salt basin. Bulletin American Association Petroleum Geologists, 91(11): 1541-1557.

Schröder, S., Amthor, J.E. and Matter, A., 2000b. Unusual hydrocarbon reservoirs in intrasalt carbonate stringers (Birba Area), Infracambrian Ara Group, S-Oman. GeoArabia, 5(1): 177.

Schröder, S., Schreiber, B.C., Amthor, J.E. and Matter, A., 2000a. Evaporites of the Ara Group (South Oman): an essential element of stratigraphy in an Infracambrian salt basin. GeoArabia, 5(1): 176-177.

Talbot, C.J., 1981. Sliding and other deformation mechanisms in a glacier of salt, S Iran. Geological Society, London, Special Publications, 9(1): 173-183.

Talbot, C.J., 1992a. Quo vadis tectonophysics? With a pinch of salt! Tectonophysics, 16(1-2): 1-20.

Talbot, C.J., 1992b. Centrifuged models of Gulf of Mexico profiles. Marine and Petroleum Geology, 9(4): 412-432.

Talbot, C.J. and Jackson, M.P.A., 1987a. Internal kinematics of salt diapirs. American Association of Petroleum Geologists Bulletin, 71: 1068–1093.

Talbot, C.J. and Jackson, M.P.A., 1987b. Salt tectonics. Scientific American, 257(2): 70-79.

Talbot, C.J., Medvedev, S., Alavi, M., Shahrivar, H. and Heidari, E., 2000. Salt extrusion at Kuh-e-Jahani, Iran, from June 1994 to November 1997. Geological Society, London, Special Publications, 174(1): 93-110.

Ter Heege, J.H., De Bresser, J.H.P. and Spiers, C.J., 2005. Dynamic recrystallisation of wet synthetic polycrystalline halite: dependence of grain size distribution on flow stress, temperature and strain. Tectonophysics, 396: 35-57.

Urai, J.L., Schléder, Z., Spiers, C.J. and Kukla, P.A., 2008. Flow and Transport Properties of Salt Rocks. In: R. Littke (Editor), Dynamics of complex intracontinental basins: The Central European Basin System. Elsevier, pp. 277-290.

Urai, J.L. and Spiers, C.J., 2007. Theeffect of grain boundary water on deformation mechanisms and rheology of rocksalt during long-term deformation. In: M. Wallner, K. Lux, W. Minkley and H. Hardy Jr. (Editors), Proceedings of the 6th conference on the mechanical behavior of salt, Hannover, Germany, May 22–25, 2007. Taylor and Francis, Basingstoke, pp. 1-9.

Urai, J.L., Spiers, C.J., Zwart, H.J. and Lister, G.S., 1986. Weakening of rock salt by water during long-term creep. Nature, 324(6097): 554-557.

Warren, J.K., 2016. Evaporites: A compendium (ISBN 978-3-319-13511-3). Springer, Berlin, 1854 pp.

Warren, J.K., 2017. Salt usually seals, but sometimes leaks: Implications for mine and cavern stabilities in the short and long term. Earth-Science Reviews, 165: 302-341.

Saltworks Consultants Pty Ltd
ABN 068 889 127
Kingston Park,
5049 South Australia

Email: enquiries@saltworkconsultants.com

Web Page: www.saltworkconsultants.com